Li Wenhui (Orcid ID: 0000-0002-3510-7081)

Relationship between the Interannual and Intraseasonal Temperature Variability in Northeast China

Wenhui Li[1,2], Guirong Tan[1], and Tim Li[3,1]

1. Key Laboratory of Meteorological Disaster, Ministry of Education (KLME) / Joint International Research Laboratory of Climate and Environmental Change (ILCEC) / Collaborative Innovation Center on Forecast and Evaluation of Meteorological Disasters (CIC-FEMD), Nanjing University of Information Science and Technology, Nanjing, 210044, China

2. Meteorological Public Service Center of Guangdong Province, Guangdong Province, Guangzhou, 510080, China

3. Department of Atmospheric Sciences, School of Ocean and Earth Science and Technology, University of Hawaii, Honolulu, Hawaii, HI96822, USA

Corresponding author: Tim Li, Department of Atmospheric Sciences, School of Ocean and Earth Science and Technology, University of Hawaii at Manoa, Honolulu, Hawaii 96822. Email: timli@hawaii. edu

This is the author manuscript accepted for publication and has undergone full peer review but has not been through the copyediting, typesetting, pagination and proofreading process, which may lead to differences between this version and the Version of Record. Please cite this article as doi: 10.1002/joc.7247

This article is protected by copyright. All rights reserved.

Author Manuscript

Author Manuscript

Abstract

A significant negative correlation between the seasonal mean temperature anomaly and the intensity of the intraseasonal temperature oscillation in the northern winter over Northeast China is found during the time period 1959-2011. A stronger intraseasonal oscillation (ISO) is found during an extremely cold winter. The cold winter in Northeast China is a part of zonally oriented large-scale pattern with a negative (positive) temperature anomaly in mid- (high) latitudes and is associated with a negative phase of the North Atlantic Oscillation (NAO). The intraseasonal temperature anomaly originates from high-latitude Central Eurasia and propagates southeastward. The southeastward propagation is attributed to the upper tropospheric dispersion of Rossby wave energy as a result of coupling of the low-level temperature and the upper-level geopotential height.

The cause of the negative correlation between the intraseasonal and interannual modes is investigated. A cold winter in Northeast China is associated with a weakened meridional temperature gradient and vertical wind shear north of 50° N. This weakens synoptic variability in situ through baroclinic instability. Because the ISO competes for an energy source with the synoptic motion, the ISO is enhanced north of 50° N. The southeastward propagation of the enhanced ISO mode increased intraseasonal temperature variability over Northeast China. As a result, a cold winter in Northeast China is accompanied by an enhanced ISO variability in situ.

The enhanced local ISO could further feed back to the winter mean temperature anomaly through nonlinear advective processes. The diagnosis of the temperature budget indicates that the ISO may interact with motion on other scales to contribute to the winter mean temperature anomaly in situ.

Keywords: intraseasonal oscillation; winter temperature anomaly; two-way interaction between intraseasonal and interannual oscillations

Author Manuscript

1. Introduction

Regional extreme abnormal climate events have occurred more frequently over China under the current conditions of global warming (Chen J Q et al, 1996; Zhang Y Q et al, 2018; Guo J P et al, 2020). Extremely cold temperature, strong snowstorms and freezing conditions (such as those in 2007-2008 and 2011-2012) have occurred intermittently in winter, greatly influencing agriculture, transportation and the economy (Wen et al, 2009; Zhou et al. 2009). The winter temperature anomaly is one of the primary targets of short-range climate predictions and is influenced not only by interannual and interdecadal variations, but also by intraseasonal oscillation (ISO) and synoptic-scale motion (Jeong 2005; Jin F F et al, 2006a, b; T. Li , 2017; Song L et al, 2017; Takaya and Nakamura 2005a, b; Song et al. 2016; Yao et al, 2016). Few studies have examined the upscale feedback of the ISO to the interannual variation.

Since Madden and Julian (1971, 1972) first discovered the tropical ISO, a number of studies have demonstrated that the ISO not only exists in the tropics (Madden and Julian 1971, 1972; Teng and Wang 2003; Wang et al, 2006), but also in mid- and high- latitude regions (Jeong et al, 2008; Yang and Tim Li, 2016). The ISO in the tropics and at higher latitudes may interact through atmospheric teleconnection patterns (Li C Y, 1990, 1991; Lin et al, 2009a, b), leading to a persistent temperature anomaly in East Asia (Zhou et al, 2005; Lin et al, 2009a, b; Zhu Y Y et al, 2013). The winter temperature anomaly exhibits a strong interannual and intraseasonal variation in addition to the pronounced synoptic scale variation (He J H et al; 2011; Jeong et al, 2005; Song L et al, 2016). The ISO might provide a large-scale background for the outbreak of synoptic cold wave events (Ma X Q et al., 2008; Miao Q et al., 2016), and may strengthen the cold wave enough to cause an extreme cold event (Jeong et al., 2005; Ren et al., 2009).

Previous studies on the intraseasonal variability of temperature at high latitudes have focused on the origin and propagation mechanism of the ISO (Yang and T. Li, 2016; Zhao C and T. Li, 2017; Yang and T. Li, 2017). How the ISO influences the interannual variability is unclear. It has been shown that the tropical ISO exerts a great impact on the interannual variability (Goswami et al. 2006; Waliser 2006; Palmer et al, 2008). This motivates us to explore the interaction between the ISO and the interannual variation in winter temperatures

Author Manuscript

at high latitudes. This study may provide a theoretical foundation for short range climate prediction.

The objective of this study is to determine the linkage between the interannual winter temperature anomaly and the intensity of the ISO. We focus on Northeast China, a region of strong interannual and intraseasonal temperature variability. The remainder of this paper is organized as follows. Section 2 describes the datasets and methods used in this study. Sections 3 and 4 describe the pattern and evolution characteristics of the intraseasonal and interannual winter temperature anomalies in Northeast China, respectively. Section 5 discusses the two-way interaction between the intraseasonal and interannual winter temperature anomalies and our conclusion are given in Section 6..

2. Data and methods

The daily surface air temperature data derived from the National Meteorological Information Center of China Meteorological Administration for 410 ground observational stations and the National Centers for Environment Prediction (NCEP) / National Center for Atmospheric Research (NCAR) reanalysis datasets (2.5˚×2.5˚) for 1959-2011 are used. The reanalysis data include the 3-dimensional temperature (T), geopotential height (Z), zonal wind (u), meridional wind (v) and vertical p-velocity (ω) at 12 pressure levels (1000, 925, 850, 700, 600, 500, 400, 300, 250, 200, 150, and 100 hPa). The 2m air temperature field from the NCEP/NCAR reanalysis is used to compare with the surface station observation. The sea surface temperature (SST) data from the Hadley Center Global Sea Ice and Sea Surface Temperature (HadISST) datasets with a resolution of 1˚×1˚ are used.

The intraseasonal timescale (10–90 day) signals are extracted by the Lanczos band-pass filter (Duchon, 1979). Before applying the band-pass filtering, the climatological annual cycle is first removed from the original data. The 10-90-day period is selected based on power spectrum analysis of the surface temperature anomaly. A Student t-test is applied to test the significance of composite, correlation and regression analyses.

We use a phase-independent wave-activity flux (WAF) formulated by Takaya and Nakamura (2001) to illustrate the propagation of Rossby wave activity associated with the intraseasonal variations of the winter temperature. A two dimensional WAF may be expressed as:

$$W = \frac{1}{2|\bar{U}|}\begin{bmatrix}\bar{u}(\psi_x'^2 - \psi'\psi_{xx}') + \bar{v}(\psi_x'\psi_y' - \psi'\psi_{xy}') \\ \bar{u}(\psi_x'\psi_y' - \psi'\psi_{xx}') + \bar{v}(\psi_x'^2 - \psi'\psi_{yy}')\end{bmatrix} \quad (1)$$

where $V = (\bar{u}, \bar{v})$ is the climatological winter mean horizontal wind field during the time period 1960-2011, ψ' denotes the perturbation streamfuction, a prime denotes the intraseasonal anomalies, and the subscripts x and y denote partial derivatives in the zonal and meridional directions, respectively.

To understand the role of multi-scale interactions in affecting the interannual anomaly of the winter temperature, a low-level heat budget analysis is conducted. The temperature equation may be written as:

$$\frac{\partial T}{\partial t} = -\vec{v} \cdot \nabla T + S\omega + \frac{Q}{c_p} \quad (2)$$

where *S* denotes the atmospheric static stability parameter and *Q* denotes diabatic heating, which can be calculated based on Yanai (1973).

3. Relationship between the winter mean temperature anomaly and the intensity of the intraseasonal temperature variability in Northeast China

The spatial distribution of the climatological winter mean surface air temperature in China shows a dipole pattern between northern and southern China (Fig. 1a). The temperature increases toward the south as a result of the impact of the East Asian winter monsoon. The 0℃ line is approximately along 32°N, passing from northern Jiangsu Province westward to northern Sichuan Province. The coldest mean temperature (about −18℃) appears over Northeast China, while the warmest temperature (14℃) appears over South China. Figure 1b shows the standard deviations of the winter (DJF) temperature anomalies during the time period 1960-2011. The standard deviation equation may be written as:

$$S = \sqrt{\frac{\sum_{i=1}^{n}(x_i - \bar{x})^2}{n}} \quad (3)$$

where *S* is the standard deviation, *x* is the winter (DJF) temperature, subscript *i* denotes the year, $\bar{x}$ is the winter (DJF) mean temperature during the time period 1960–2011 and *n* is the total number of years. Figure 1b shows a maximum winter temperature variability center located over northern China. The combination of Figure 1a and 1b indicates that the region of both maximum mean cooling and maximum interannual variability is in northern China.

Author Manuscript

Author Manuscript

To examine the relative contribution of the interannual variability to the total temperature variability, Figure 1c shows the standard deviation map of the non-filtered temperature anomaly (i.e., only the climatological annual cycle is removed from the raw data). First, we calculate the standard deviation of the non-filtered daily temperature anomalies each year and then averaged this for the time period 1960–2011. This shows that the interannual component only explains a small portion of the total temperature variability. This prompts us to examine the sub-seasonal (or intraseasonal) temperature variability. Figure 1d shows the mean distribution of standard deviation of 10-90-day filtered temperature anomalies for the time period 1960-2011. It is obvious that the intensity of the intraseasonal temperature oscillation is much greater than that of the interannual counterpart. In fact, the intraseasonal temperature variability explains about 60% of the total variability.

Figure 1d shows four centers of maximum variability located over Northeast, Northwest, North and South China. By calculating the correlation coefficients between the ISO intensity in the four centers and the winter mean temperature anomaly in other regions across China (not shown), we note that there are negative correlations in all centers, but they are not always statistically significant. The strongest and statistically significant negative correlation occurs in Northeast China, which is why this study focuses on the relationship between the ISO intensity and the winter mean temperature anomalies in Northeast China.

This analysis is consistent with the results obtained using the NCEP/NCAR reanalysis datasets (not shown). We conclude that maximum winter temperature variabilities occurs on intraseasonal and interannual timescales in Northeast China and the intraseasonal variability is much greater than the interannual variability.

To test the sensitivity of these results for different data periods, we conduct a parallel calculation using the NCEP/NCAR reanalysis product with the data extended to 2020. The result is similar, suggesting that the winter temperature variabilities on intraseasonal and interannual timescales are robust.

To illustrate the spatial patterns of the interannual and intraseasonal variability modes over Northeast China, we select a reference point, Huma Station (51.43°N, 126.39°E), where both the interannual and intraseasonal variabilities are strong. Figure 2a shows a map of the correlation between the time series of the winter mean (DJF) temperature anomaly at Huma and

other stations for the time period 1960-2011. The correlation coefficient equation may be written as:

$$r = \frac{\frac{1}{n}\sum_{i=1}^{n}(x_i - \bar{x})^2 (y_i - \bar{y})^2}{\sqrt{\frac{\sum_{i=1}^{n}(x_i - \bar{x})^2}{n}}\sqrt{\frac{\sum_{i=1}^{n}(y_i - \bar{y})^2}{n}}} \quad (4)$$

where *r* denotes the correlation coefficient, *x* and *y* denote the winter (DJF) temperature of Huma station and all other stations, the subscript *i* denotes the year, $\bar{x}$, $\bar{y}$ denotes the winter (DJF) mean temperature of Huma station and all other stations during the time period 1960–2011 and *n* is the total number of years. We also calculate the correlation map between the time series of the ISO intensity each year at Huma and other stations for the time period 1960-2011 (Fig. 2b). Here, *x* and *y* denote the ISO intensity at Huma and other stations, the subscript *i* denotes the year, $\bar{x}$, $\bar{y}$ denotes the mean ISO intensity at Huma and other stations during the time period 1960–2011 and *n* is the total number of years. Significant positive correlations appear over Northeast China. This indicates that the interannual temperature variability is on a large scale, covering entire Northeast China and beyond. This is why we can use the box-averaged temperature index over the region (38-53° N, 118-133° E, the black box in Figure 2) to represent the interannual and intraseasonal temperature variabilities over Northeast China.

Figure 3a shows the correlation map between the time series of the ISO intensity averaged over 38-53° N, 118-133° E and the time series of the winter temperature anomaly at all stations. Significant negative correlations appear over Northeast China. Figure 3b illustrates the time series of the box-averaged winter temperature anomaly and ISO intensity averaged over 38-53° N, 118-133° E. The correlation coefficient between them is -0.32, exceeding the 95% confidence level. This implies that a stronger (weaker) ISO variability is often accompanied by a cold (warm) winter over Northeast China.

To illustrate the relative contributions of the interannual and interdecadal components, we remove a 6-year running mean form the original temperature time series to obtain the ″pure″ interannual signal and then calculate the correlation coefficient between the interannual time series of the winter temperature anomaly and the ISO intensity. The correlation coefficient is -

Author Manuscript

Author Manuscript

0.28, still exceeding the 95% confidence level. This indicates that the significant negative correlation between the winter mean temperature anomaly and the ISO intensity in Northeast China is primarily attributed to their interannual component.

The blue solid and dotted lines in Figure 3b represent the normalized 10-90-day filtered temperature variability averaged over the key region from the reanalysis and stations datasets, respectively. The red solid and dotted lines represent the normalized winter temperature anomalies over the same region from the reanalysis and stations datasets, respectively. The correlation coefficients between the red solid and dotted lines and between the blue solid and dotted lines both exceed 0.9. Both the ISO intensity and the winter temperature anomaly exhibit a strong interannual variation in the region.

The time series of the standardized winter temperature anomaly shown in Figure 3b is used to classify typical cold and warm events in Northeast China during the time period 1960-2011, with values greater than 1 (less than -1) being selected as a cold (warm) winter. Nine cold (1966, 1969, 1977, 1985, 1986, 2001, 2006, 2010, and 2011) and nine warm (1962, 1973, 1982, 1983, 1989, 1999, 2002, 2004, and 2007) winters are selected. To identify the dominant periods of the ISO for the selected cold or warm winters, a power spectral analysis is applied. Figure 3c and 3d show that the dominant ISO periods are, in general, in the band 10-40 days in both cold and warm winters, with maximum spectrum power shifting slightly toward a longer period during the cold winters.

4. Origin and structure of the intraseasonal temperature variability in Northeast China

We investigate the origin of the ISO to try to explain the exceptionally strong intraseasonal temperature variability in Northeast China. A lead-lag regression analysis is conducted to reveal the structure and evolution of the intraseasonal temperature anomaly. Figure 4 shows the evolution of the 10−90-day filtered 2m air temperature and geopotential height fields at 300 hPa from day −9 to day 0 in cold (Fig. 4a) and warm (Fig. 4b) winters. The blue and red dots represent maximum positive temperature and geopotential height anomaly centers, respectively.

Regardless of whether the winter is cold or warm, the intraseasonal temperature variability in Northeast China originates from high-latitude Central Asia. A positive temperature anomaly appears at the northwest of Baikal Lake on day −9. The intraseasonal temperature perturbation then moves gradually southeastward. An upper level positive geopotential height anomaly is

Author Manuscript

associated with the positive surface temperature perturbation. The centers of both the positive temperature and geopotential height anomalies propagate southeastward and reach Northeast China on day 0. This indicates that the low-level intraseasonal temperature anomalies are closely associated with the upper-tropospheric height signal.

Figure 5a and 5b show the tracks of the regressed temperature (blue dots) and geopotential height (red dots) centers from day −9 to day 0 for cold and warm winters. Both panels clearly exhibit a southeastward propagation track, with a more northwestward tilt in warm winters. We hypothesize that the southeastward propagation of the upper tropospheric geopotential height is a result of the propagation of Rossby wave energy. We therefore calculate the Rossby wave activity flux (WAF) at 300 hPa using the 10–90-day filtered data from day –9 to day 0. The WAF formula used here is a phase-independent WAF developed by Takaya and Nakamura (2001). The WAF field calculated in this way is plotted in Figure 5c and 5d. There are pronounced southeastward wave activity fluxes over high-latitude Eurasia in both cold and warm winters, confirming that the dispersion of Rossby wave energy is a major cause of the southeastward propagating geopotential height in the upper troposphere. In other words, the upper-tropospheric wave train shown in Figure 4 is likely a result of the propagation of Rossby wave energy.

To illustrate the vertical structure of the ISO mode, we plot the vertical-horizontal profiles of the 10–90-day filtered geopotential height and temperature anomalies along the yellow line at day 0. Figure 6 shows that the maximum temperature anomaly appears near the surface, whereas the maximum geopotential height anomaly appears at 300 hPa. A warm anomaly below and a cold anomaly above 300 hPa are accompanied by a positive geopotential height anomaly center at 300 hPa, implying a hydrostatic relationship. Given the close relationship between the low-level temperature and upper-tropospheric geopotential height fields, the propagation of Rossby wave energy may be regarded as a mechanism for the southeastward movement of the intraseasonal near-surface temperature perturbation.

5. Two-way interactions between the interannual and intraseasonal temperature variability

The significant negative correlation between the winter temperature anomaly and the ISO strength shown in Figure 3b suggests a possible impact of the interannual background state on

Author Manuscript

the intraseasonal variability. Figure 7 shows the differences in temperature, geopotential height and wind anomalies between cold and warm winters at 700, 500 and 300 hPa. Zonally oriented large-scale cold (warm) anomalies over mid-(high) latitudes accompanied the cold winters in Northeast China. This indicates that the cold Northeast China is only a part of the large-scale cooling across a large portion of mid-latitude zone between 30°N-60°N. The temperature anomalies exhibit an equivalent barotropic structure throughout the troposphere. The cold anomalies at mid-latitudes are accompanied by large-scale cyclonic and low pressure anomalies, whereas the warm anomalies at high-latitudes are accompanied by large-scale anticyclonic and high pressure anomalies.

A positive geopotential height anomaly over Ural Mountain is associated with a negative phase of the North Atlantic Oscillation (NAO) in North Atlantic region. Previous studies have suggested that the high pressure in the Ural Mountains is strengthened during the negative phase of the NAO, which could promote downstream-propagating Rossby wave activity and cause frequent cold events in Northeast China (Hurrell, 1996; Sun C et al,2012; Fan k et al, 2013; Li C et al, 2015). Cold winters in Northeast China may therefore be related to forcing from the North Atlantic.

Figure 8 shows the differences in composite diabatic heating and SST fields between cold and warm winters. A dipole heating pattern appears in the North Atlantic sector. A cold (warm) SST anomaly in the mid- (high) latitude Atlantic implies an enhanced (weakened) surface latent heat flux and thus a positive (negative) lower tropospheric heating anomaly. The latter further induces the negative NAO pattern.

An interesting question is how the change in the background state associated with the interannual temperature variability affects the strength of the ISO. We speculate that it is through the modulation of the Westerly Jet. Figure 9a illustrates the distributions with latitude of the vertically integrated (850-300 hPa) temperature anomaly and vertical shear of zonal winds between 200 and 850 hPa, averaged between 80 and 120°E, for the cold minus warm winter composite. An enhanced (weakened) meridional temperature gradient appears south (north) of 50° N. This led to a strengthening (weakening) of the vertical shear south (north) of 50° N as a result of the thermal wind relation. The strengthened (weakened) vertical shear favored (prohibited) the growth of local synoptic（<10 days）perturbations, through the

modulation of the baroclinic instability. Figure 9b confirms that the synoptic variability is indeed stronger (weaker) south (north) of 50° N.

The intensity of the ISO is opposite to that of the synoptic variability (Fig. 9b). Physically, it is argued that the ISO may compete with synoptic motion for source of energy. As a result, the ISO is enhanced north of 50° N during the cold winters. The southeastward propagation of the enhanced ISO further increased the intraseasonal variability over Northeast China.

The strengthened ISO variability may feed back to the winter mean temperature anomaly in Northeast China through a nonlinear rectification process. The temperature equation refers to Equation(2), where $\vec{V}$ denotes horizontal wind vector, ω is the p-vertical velocity, ∇ is the horizontal gradient operator, $S = \frac{\alpha}{c_p} - \frac{\partial T}{\partial p}$ is the atmospheric stability parameters, α is the specific volume of air, Cp is the specific heat of air and Q is the rate of diabatic heating. The other symbols follow convention in meteorology. The interannual temperature equation can therefore be expressed as:

$$\frac{\partial \mathrm{T_j}}{\partial \mathrm{t}} = -(\vec{\mathrm{V}} \cdot \nabla \mathrm{T})_\mathrm{j} + (\mathrm{S}\omega)_\mathrm{j} + \frac{\mathrm{Q_j}}{\mathrm{C_p}} \qquad (5)$$

where $(\,)_\mathrm{j}$ represents the interannual component. If we let Δ be the difference between cold and warm winters and assume that the interannual temperature tendency vanishes during extreme cold and warm winters (i.e., $\frac{\partial \mathrm{T_j}}{\partial \mathrm{t}}$=0), then we can derive the following equation:

$$0 = \Delta(\vec{\mathrm{V}} \cdot \nabla \mathrm{T})_\mathrm{j} - \Delta(\mathrm{S}\omega)_\mathrm{j} - \frac{\Delta \mathrm{Q_j}}{\mathrm{C_p}} \qquad (6)$$

In equation (6), the apparent heat source *Q* can be calculated from the original reanalysis field by applying this equation to 1000 hPa and assuming that the diabatic heating near the surface is primarily determined by longwave radiative cooling and surface heat flux. For simplicity, we can set $\Delta \mathrm{Q_j} = \gamma \cdot \Delta \mathrm{T_j}$, where $\gamma = \frac{\partial \mathrm{Q_j}}{\partial \mathrm{T_j}}$ represents the dependence of the diabatic heating on local temperature, which can be determined by fitting the observed relationship between $\mathrm{T_j}$ and $\mathrm{Q_j}$ during the analysis period (1960-2011).

The winter mean temperature difference between the cold and warm years can be therefore be determined by

$$\Delta \mathrm{T_j} = \frac{\mathrm{C_p}}{\gamma}\left[\Delta\left(\vec{\mathrm{V}} \cdot \nabla \mathrm{T}\right)_\mathrm{j} - \Delta(\mathrm{S}\omega)_\mathrm{j}\right] \qquad (7)$$

Author Manuscript

Author Manuscript

Figure 10 is a scatter diagram between the winter mean temperature and diabatic heating anomalies at 1000 hPa averaged over Northeast China (box region). A negative slope ($\Delta Q_j = -0.3 * \Delta T_j$) indicates a negative correlation between the temperature anomaly and the heating anomaly. The linear fit is statistically significant, exceeding the 95% confidence level. Equation (7) may be rewritten as

$$\Delta T_j = \frac{10Cp}{3}\left[\Delta(-\vec{v}\cdot\nabla T)_j + \Delta(S\omega)_j\right] \quad (8)$$

Given the nonlinear nature of the two terms on the right hand side, Equation (8) can be used to assess the relative contributions to the winter temperature anomaly by the interannual flow alone and by multi-scale interaction processes. Before assessing the nonlinear rectification process, we first examine the relative roles of the horizontal advection versus the adiabatic term for both cold and warm winters separately. Table 1 shows the results of the calculation. Here Δ denotes the cold or warm winter composite minus the long-term climatology. Table 1 shows that the average winter temperature anomaly is -1.9 K for the cold winter composite. The sum of the horizontal advection and the adiabatic term on the right hand side of Equation (8) is -1.8 K, indicating the budget is approximately balanced. The horizontal advection term plays a major role and accounts for 71% of cooling.

For the warm winter composite, the average temperature anomaly is 1.7 K, whereas the sum of the horizontal advection and the adiabatic term on the right hand side of Equation (8) is 1.6 K. The horizontal temperature advection accounts for 84% of the anomalous warm temperature in winter. The analysis of both cold and warm winters therefore indicates that the interannual variation of the winter surface air temperature in Northeast China is primarily controlled by anomalous horizontal temperature advection. Equation (8) captures well the year-to-year change in the winter temperature in Northeast China.

Given that Equation (8) is able to capture the observed winter temperature change, we examine the relative contribution of the nonlinear rectification effect. Each dependent variable in Equation (8) is separated into four components, a climatological winter mean component (denoted by subscript c), an interannual component (> 90 days, denoted by subscript j), an intraseasonal component (10–90 days, denoted by subscript i) and a synoptic-sale component (<10 days, denoted by subscript e). The horizontal advection and adiabatic terms may therefore

be decomposed into 16 terms:

$$\left(\overline{-\vec{V}\cdot\nabla T}\right)_j = \left[-\vec{V}_i\cdot\nabla T_i\right]_j + \left[\overline{-\vec{V}_i}\cdot\nabla(T_c+T_j+T_e)\right]_j + \left[-(\vec{V}_c+\vec{V}_j+\vec{V}_e)\cdot\nabla T_i\right]_j$$
$$+\left[-(\vec{V}_c+\vec{V}_j+\vec{V}_e)\cdot\nabla(T_c+T_j+T_e)\right]_j \quad (9)$$

$$(S\omega)_j = (S_i\omega_i)_j + \left[S_i\cdot(\omega_c+\omega_j+\omega_e)\right]_j + \left[(S_c+S_j+S_e)\cdot\omega_i\right]_j$$
$$+\left[(S_c+S_j+S_e)\cdot(\omega_c+\omega_j+\omega_e)\right]_j \quad (10)$$

where the first term on the right hand side of Equations (9) and (10) represents the effect of eddy-eddy interaction associated with the ISO and the second and the third terms represent the influence of the ISO interacting with other scale motions. The sum of the first three terms in Equations (9) and (10) is called A1 and B1, representing the overall impact of the ISO. The fourth term on the right hand side of Equation (9) represents the influence of the scale interactions among other scales beyond the ISO, which includes the advection of anomalous temperature by the mean flow $\left[-\Delta\left(\vec{V}_c\cdot\nabla T_j\right)_j\right]$ (term A21), the advection of the mean temperature by anomalous wind $-\Delta[(\vec{v}_j\cdot\nabla T_c)_j]$ (term A22) and the sum of the remaining horizontal advection terms (term A23). The fourth term on the right hand side of Equation (10) consists of $[\Delta\left(S_c\omega_j\right)_j]$ (term B21), $[\Delta\left(S_j\omega_c\right)_j]$ (term B22) and the sum of the remaining adiabatic terms (term B23).

The relative contributions of the individual terms in Equations (9) and (10) to the temperature anomalies during cold and warm winters are shown in Figure 11. As expected, the winter temperature anomaly during cold and warm winters is primarily attributed to the interaction between the climatological mean and the interannual component. For both the cold and warm winter composites, the largest two terms are the horizontal advection of the interannual temperature anomaly by the climatological mean wind $[-\Delta\left(\vec{V}_c\cdot\nabla T_j\right)_j]$and the horizontal advection of the climatological mean temperature by the interannual wind$-\Delta[(\vec{v}_j\cdot\nabla T_c)_j]$. They account on average for 60% of the winter temperature anomalies. Additional contributions arise from the adiabatic terms associated with the interannual vertical velocity $[\Delta\left(S_c\omega_j\right)_j]$ and the interannual atmosphere stability anomaly $[\Delta\left(S_j\omega_c\right)_j]$. These

Author Manuscript

Author Manuscript

contributions account for about 15% of the changes in interannual temperature. The ISO related multi-scale interaction process (i.e., the first 3 terms on the right hand side of Equation (9) and (10)) contributes positively to the interannual temperature anomaly, suggesting that there exists a positive feedback between the local intraseasonal and interannual modes. A cold winter promotes a stronger ISO activity, which further strengthens the cold anomaly through the nonlinear temperature advection. The ISO related nonlinear rectification accounts for 10-20% of the seasonal mean temperature anomaly during cold and warm winters.

The processes that contribute to the anomalous horizontal temperature advection may be understood from Figure 12, which shows the horizontal patterns of the climatological mean and anomalous temperature and wind fields at 1000 hPa. In the northern winter, the climatological mean wind is northwesterly in the key analysis region. For cold winters, the maximum interannual temperature anomaly center is located north of Baikal, northwest of Northeast China. As a result, there is pronounced anomalous cold advection into the key analysis region (Fig. 12a) and an anomalous northerly over Northeast China. The climatological mean temperature decreases with the increased latitude (Fig. 12b). The anomalous northerly transport the cold mean temperature southward, causing a cold winter in Northeast China.

6. Summary and discussion

The interannual variation of the winter surface air temperature in Northeast China displays a significant negative correlation with the intensity of the intraseasonal temperature variability in situ. A cold (warm) winter is often accompanied with the local stronger (weaker) ISO variability. Both the ISO intensity and the winter mean temperature anomaly exhibit a strong interannual variation.

The origin of the intraseasonl temperature variability is examined. The near surface temperature perturbation is accompanied by the upper-tropospheric geopotential height anomaly, and both the anomalies are originated from northwest of Northeast China, moving southeastward. The southeastward propagation of the upper-tropospheric geopotential height anomaly is a result of the propagation of Rossby wave energy, as confirmed by the composite Rossby WAF field at 3 00hPa. The dispersion of Rossby wave energy is therefore a major mechanism for the southeastward propagating of the geopotential height in the upper troposphere. The vertical profiles of the intraseasonal geopotential height and temperature

anomalies show a hydrostatic relationship between a maximum positive (negative) geopotential height anomaly at 300 hPa and a warm (cold) temperature anomaly center near the surface. Such a close relation implies that the southeastward movement of the near surface temperature perturbation is likely a result of the Rossby WAF in the upper troposphere.

The cold winter mean temperature anomaly in Northeast China is associated with a zonally oriented large-scale temperature pattern in Eurasia with a negative (positive) temperature anomaly and a cyclonic (anticyclonic) circulation anomaly covering the mid- (high) latitudes. It is accompanied by a negative phase of the North Atlantic Oscillation. A mirror image of the circulation pattern appears in the warm winter composite. The enhanced (weakened) temperature gradient south (north) of 50° N during cold winters strengthened (weakened) the local vertical westerly wind shear, favoring (prohibiting) the development of a synoptic perturbation through the strengthened (weakened) baroclinic instability. Because the ISO competes for an energy source with the synoptic motion, the ISO is enhanced north of 50° N. The southeastward propagation of the enhanced ISO increased intraseasonal variability over Northeast China. The cold winter mean temperature anomaly in Northeast China is therefore associated with an enhanced intraseasonal variability in situ.

The strengthened ISO perturbation in Northeast China during cold winters may feed back to the interannual temperature anomaly through nonlinear advective processes. A theoretical model for understanding the interannual temperature variation is constructed. The diagnosis of the cold and warm temperature anomalies indicates that the main contributors are the advection of the climatological mean temperature by the interannual wind anomaly and the advection of the interannual temperature anomaly by the climatological mean wind. The adiabatic term also make a positive contribution. It is interesting to note that the ISO, through its nonlinear interaction with other scale motions, contributes positively to the interannual temperature anomaly in boreal winter.

The results of the observational analysis imply a positive two-way interaction between the interannual temperature anomaly and the strength of the ISO. A cold winter in Northeast China induces enhanced (weakened) temperature gradient and vertical wind shear south (north) of 50° N. This promotes a strengthened synoptic-scale variability (ISO activity) south (north) of 50°

Author Manuscript

N. The southeastward propagation of the enhanced ISO increased the intraseasonal variability over Northeast China, which may strengthen the anomalous cold winter mean temperature. These results may provide a new avenue for understanding and predicting the seasonal mean temperature anomaly and its relationship with subseasonal temperature change at high latitudes. The factors revealed by the current study may provide an observational basis for short-range climate prediction and disaster prevention and mitigation.

Acknowledgements: This study is supported by NSFC grants 42088101, 41875069 and U1902209, NSF grant AGS-20-06553, and NOAA grant NA18OAR4310298. This is SOEST contribution number 12345, IPRC contribution number 1234 and ESMC number 123.

Author Manuscript

Author Manuscript

References

Chen J Q, Shi N (1996) The preliminary study on possible scenarios of flood and drought in china in the case of global warming. Chinese Geographical Science 6:145-154

Duchon C (1979) Lanczos filtering in one and two dimensions. J Appl Meteorol 18:1016–1022

Fan K，Liu H (2013) winter temperature over east Asia and atmospheric circulation patterns in the last 100 years. Chinese Journal of Atmospheric Sciences，37(2): 383-394.

Guo J P, Yan Y, Chen D D (2020) The response of warm-season precipitation extremes in China to global warming: an observational perspective from radiosonde measurements. Climate Dynamics

Goswami B. N.,G. Wu,T.Yasunari (2006) Annual cycle,intraseasonal oscillations and roadblock toseasonal predictability of the Asian summer monsoon. Jouranl of Climate,19: 5078-5099.

He J H, Lin H, Wu Z W (2011) Another look at influences of the Madden-Julian Oscillation on the wintertime East Asian weather. Journal of Geophysical Research Atmosphere 116(D3)

Hurrell J W, 1996. Influence of variations in extratropical wintertime teleconnections on Northern Hemisphere temperature. Geophys. Res. Lett., 23(6): 665-668

Jin, F.F., L.L. Pan, and M. Watanabe (2006a): Dynamics of Synoptic Eddy and Low-Frequency Flow(SELF) Interaction. Part I: A Linear Closure. J. Atmos. Sci., 63: 1677–1694.

Jin, F.F., L.L. Pan, and M. Watanabe (2006b): Dynamics of Synoptic Eddy and Low- Frequency Flow(SELF) Interaction. Part II: A Theory for Low-Frequency Modes. J. Atmos.Sci., 63:1695–1708.

Jeong J-H, Ho C-H, Kim B-M, Kwon W-T (2005) Influence of the Madden-Julian Oscillation on wintertime surface air temperature and cold surges in east Asia. J Geophys Res: Atmos 110:D11104. doi:10.1029/2004JD005408

Jeong JH, Kim BM, Ho CH, Noh YH (2008) Systematic variation in wintertime precipitation in East Asia by MJO-induced extratropical vertical motion. J Clim 21:788–801

Li C, Zhang Q Y, (2015) An observed connection between wintertime temperature anomalies over Northwest China and weather regime transitions in North Atlantic. Journal of Meteorological Research 29: 201-213

Li C Y (1990) Interaction between anomalous winter monsoon in East Asia and El NINO events.

Author Manuscript

Adv.Atmos.Sci. 7: 36-46.

Li C Y (1991) Global characteristics of 30-60 day atmospheric oscillation. Chinese Journal of Atmospheric Sciences 15: 66-76(in Chinese).

Lin H, Gilbert Brunet, Jacques Derome (2009a) An Observed Connection between the North Atlantic Oscillation and theMadden-Julian Oscillation. Journal of Climate, 22: 364-380.

Lin H, Gilbert Brunet (2009b) The Influence of the Madden-Julian Oscillation on Canadian Wintertime Surface Air Temperature. Monthly Weather Review 137: 2250-2262.

Ma X Q, Ding Y H, Xu H M et al. (2008) The relation between strong cold waves and low-frequency waves during the winter of 2004/2005. Chinese Journal of Atmospheric Sciences 32: 380-394(in Chinese).

Miao Q, Gong Y F, Deng R J et al. (2016) Impacts of the low-frequency of the low-frequency oscillation over the extra-tropics of the Northern Hemisphere on the extreme low temperature event in Northeast China in the winter of 2012/2013. Chinese Journal of Atmospheric Sciences 40: 817−830 (in Chinese)

Madden RA, Julian PR (1971) Detection of a 40–50 day oscillation in zonal wind in tropical Pacific. J Atmos Sci 28: 702–708

Madden RA, Julian PR (1972) Description of global-scale circulation cells in the Tropics with a 40–50 day period. J Atmos Sci 29: 1109–1123

Palmer.T N, Doblas-Reyes. F. J., Weisheimer. A, et al. (2008) Toward seamless prediction: Calibration of climate change projections using seasonal forecasts[J]. Bulletin of theAmerican Meteorological Society,89(04):459–470

Ren H L, Jin F F, Jong-Seong Kug, et al. (2009) A kinematic mechanism for positive feedback between synoptic eddies and NAO. Geophysical Research Letters, 36(11).

Song L, Wang L, Chen W, Zhang Y (2016) Intraseasonal variation of the strength of the East Asian trough and its climatic impacts in boreal winter. J Clim 29: 2557–2577

Song L , Wu R , Jiao Y (2017) Relative contributions of synoptic and intraseasonal variations to strong cold events over eastern China. Climate Dynamics.

Sun C, Li J P , 2012. Analysis of anomalously low surface air temperature in the Northern Hemisphere during 2009/2010 winter. Climatic and Environmental Research , 17(3): 259-

Author Manuscript

273.

Takaya K, Nakamura H (2005a) Mechanisms of intraseasonal amplification of the cold Siberian high. J Atmos Sci 62:4423–4440

Takaya K, Nakamura H (2005b) Geographical dependence of upper-level blocking formation associated with intraseasonal amplification of the Siberian high. J Atmos Sci 62:4441–4449

Teng H, Wang B (2003) Interannual variations of the boreal summer intraseasonal oscillation in the Asian-Pacific region. J Clim 16: 3572–3584

Tim Li. and P.-C. Hsu (2017) Fundamentals of Tropical Climate Dynamics, Springer, ISBN 978-3-319-59595-5.

Takaya K, Nakamura H. A formulation of a phase-Independent wave-activity flux for stationary and migratory quasigeostrophic ed-dies on a zonally varying basic flow. J Atmos Sci, 2001, 58(6): 608-627.

Wang B, Webster P, Kikuchi K, Yasunari T, Qi Y (2006) Boreal summer quasi-monthly oscillation in the global tropics. Clim Dyn 27:661–675

Waliser, D. E.,2006. Intraseasonal variability. The Asian Monsoon.Springer Berlin Heidelberg, 203–257.

Wen M, Yang S, Kumar A, Zhang P (2009) An analysis of the large-scale climate anomalies associated with the snowstorms affecting China in January 2008. Mon Weather Rev 137:1111–1131

Yao S, Sun Q, Huang Q, Chu P (2016) The 10–30-day intraseasonal variation of the East Asian winter monsoon: The temperature mode. Dyn Atmos Ocean 75:91–101

Yang S, Tim Li (2016) Intraseasonal variability of air temperature over the mid-high latitude Eurasia in boreal winter. Clim Dyn 47:2155–2175

Yang S, Li T (2016) Intraseasonal variability of air temperature over the mid-high latitude Eurasia in boreal winter. Clim Dyn 47:2155–2175

Yang, S.-Y., and T. Li (2017) The Role of Intraseasonal Variability at Mid-High Latitudes in Regulating Pacific Blockings during Boreal Winter. International Journal of Climatology, 37 (S1), 1248-1256, doi:10.1002/joc.5080.

Yanai M, Esbensen S, Chu J H. 1973. Determination of bulk properties of tropical cloud clusters from large-scale heat and moisture budget [J]. J. Atmos. Sci., 30 (4): 611-627.

Author Manuscript

Zhang Y Q, You Q L, Mao G X , et al. (2018) Short-term concurrent drought and heatwave frequency with 1.5 and 2.0°C global warming in humid subtropical basins: a case study in the Gan River Basin, China. Climate Dynamics. 52: 4621-4641.

Zhou W, Chan JCL, Chen W, Ling J, Pinto JG, Shao Y (2009) Synoptic-scale controls of persistent low temperature and icy weather over Southern China in January 2008. Mon Weather Rev 137:3978–399.

Zhu Y Y, Jiang J (2013) The intraseasonal characteristics of wintertime persistent cold anomaly in China and the role of low frequency oscillation in the low latitude and midlatitude. Journal of Tropical Meteorology 29: 649-655(in Chinese)

Zhou S, Miller A J (2005). The Interaction of the Madden-Julian Oscillation and the Arctic Oscillation.Journal ofClimate, 18: 143-159

Zhao C, T. Li, Yao S X, et al. (2017) Intraseasonal Variability of Air Temperature Over East Asia in Boreal Summer. Frontiers in Earth Science 5: 63-74

Fig. 1. (a) Distribution of the climatological mean winter (DJF) temperature in the time period 1960-2011 (unit: ℃). (b) Standard deviation of the winter (DJF) temperature anomaly during the time period 1960-2011 (unit: ℃), the dots represent a standard deviation >1.5. (c) Standard deviation of the non-filtered temperature anomalies in winter (unit: ℃). (d) Standard deviation of the 10-90-day filtered temperature anomalies in winter (unit: ℃), the dots represent values >3.0.

Fig. 2. (a) Distribution of correlation coefficients between the winter temperature anomaly at the reference station (Huma) and the anomaly at other stations. (b) Distribution of the correlation coefficients between the ISO intensity in Huma and at other stations. The black dots indicate the t-test values exceeding the 95% confidence level.

Fig. 3. (a) Distribution of the correlation coefficients between the ISO intensity at the reference station (Huma) and the winter temperature anomaly at other stations in China. (b) Time series of the standardized 10-90-day filtered temperature in Northeast China using the grid (blue solid line) and station (blue dotted line) data and standardized winter temperature anomalies in

Author Manuscript

Northeast China using the grid (red solid line) and station (red dotted line) data. (c, d) Power spectrums of the 10-90-day filtered temperature averaged over Northeast China during cold and warm winters (the red line indicates the red noise spectrum and the blue dashed line indicates the 95% confidence level).

Fig. 4. Evolution (3-day interval) of the 2m temperature (shading) and 1000 hPa geopotential height (contour) fields regressed onto the 10-90-day filtered 2m temperature anomaly averaged over Northeast China from day -9 to day 0 in cold (a) and warm (b) winters. The blue and red dots denote the temperature and height centers, their latitude and longitude locations are shown in the right and left bottom corners of each panel.

Fig. 5. (Upper panel) Tracks of the regression 10-90-day filtered 2m temperature (blue dots) and geopotential height (red dots) centers from day -9 to day 0 in cold (a) and warm (b) winters. The yellow lines are linear fits of the blue curves. (Bottom panel) Composite patterns of the Rossby WAF (unit: m^2s^{-2}) at 300 hPa averaged from day -9 to day 0 during cold (c) and warm (d) winters.

Fig. 6. The vertical-horizontal cross-sections of the regressed 10-90-day filtered temperature (shading) and geopotential height (contours) anomalies along the yellow line shown in Fig. 5 at day 0 for cold (a) and warm (b) winters.

Fig. 7. Differences in temperature (shading), geopotential height (contours) and wind fields between cold and warm winters. The shading and contours exceeding the 95% confidence level. Yellow box denotes Northeast China.

Fig. 8. Differences in the diabatic heating fields at 700 hPa (a) and 400 hPa (b) and the SST field (c) between cold and warm winters. The black dots denote the region exceeding the 95% confidence level. The black box represents Northeast China.

Fig. 9. The latitude distributions of (a) vertically integrated (850-300 hPa) temperature and the

Author Manuscript

vertical shear of the zonal wind (200 hPa minus 850 hPa) anomalies and (b) standard deviations of the synoptic and intraseasonal meridional wind anomalies averaged between 80° E and 120° E for the cold minus warm winter composite.

Fig. 10. Scatter diagram of the winter temperature anomaly and the apparent heating anomaly at 1000 hPa averaged over Northeast China from 1960 to 2011. X-axis is the temperature anomaly and Y-axis is the apparent heating anomaly. The linear regression exceeds the 95% significance level.

Fig. 11. Contributions of the individual terms of Equation (8) to the 1000 hPa temperature anomaly in Northeast China averaged during cold (a) and warm (b) winters. A is the average winter temperature anomaly. A1and B1 represent the ISO related nonlinear rectification of Equations(9) and (10). A21 is $[-\Delta(\vec{V}_c \cdot \nabla T_j)_j]$and A22 is $-\Delta[(\vec{v}_j \cdot \nabla T_c)_j]$. B21 is $[\Delta(S_c\omega_j)_j]$ and B22 is $[\Delta(S_j\omega_c)_j]$. A23 is the sum of other horizontal advection. B23 is the sum of other adiabatic terms.

Fig. 12. (a) Horizontal distribution of the interannual temperature anomaly (shading) and the climatological mean wind (vectors) at 1000 hPa. (b) Horizontal distribution of the interannual wind anomaly (vectors) and the climatological mean temperature (shading) at 1000 hPa. Black box denotes the key analysis region over Northeast China. The anomalies are the differences between cold and warm winters.

Table 1. The average winter temperature anomaly (unit: K) and the contributions from the horizontal advection, the adiabatic term and summation of the two terms at 1000 hPa in cold (left) and warm (right) winters in Northeast China

	Cold Winter Composite	Warm Winter Composite
Temperature anomaly	-1.9	1.7
Horizontal advection	-1.4	1.4
Adiabatic term	-0.4	0.2

Sum of horizontal advection and adiabatic terms	-1.8	1.6

Author Manuscript

Author Manuscript

Author Manuscript

Author Manuscript

Author Manuscript

Author Manuscript

Author Manuscript

Author Manuscript

Author Manuscript

Author Manuscript

Author Manuscript

Author Manuscript

Author Manuscript

Author Manuscript

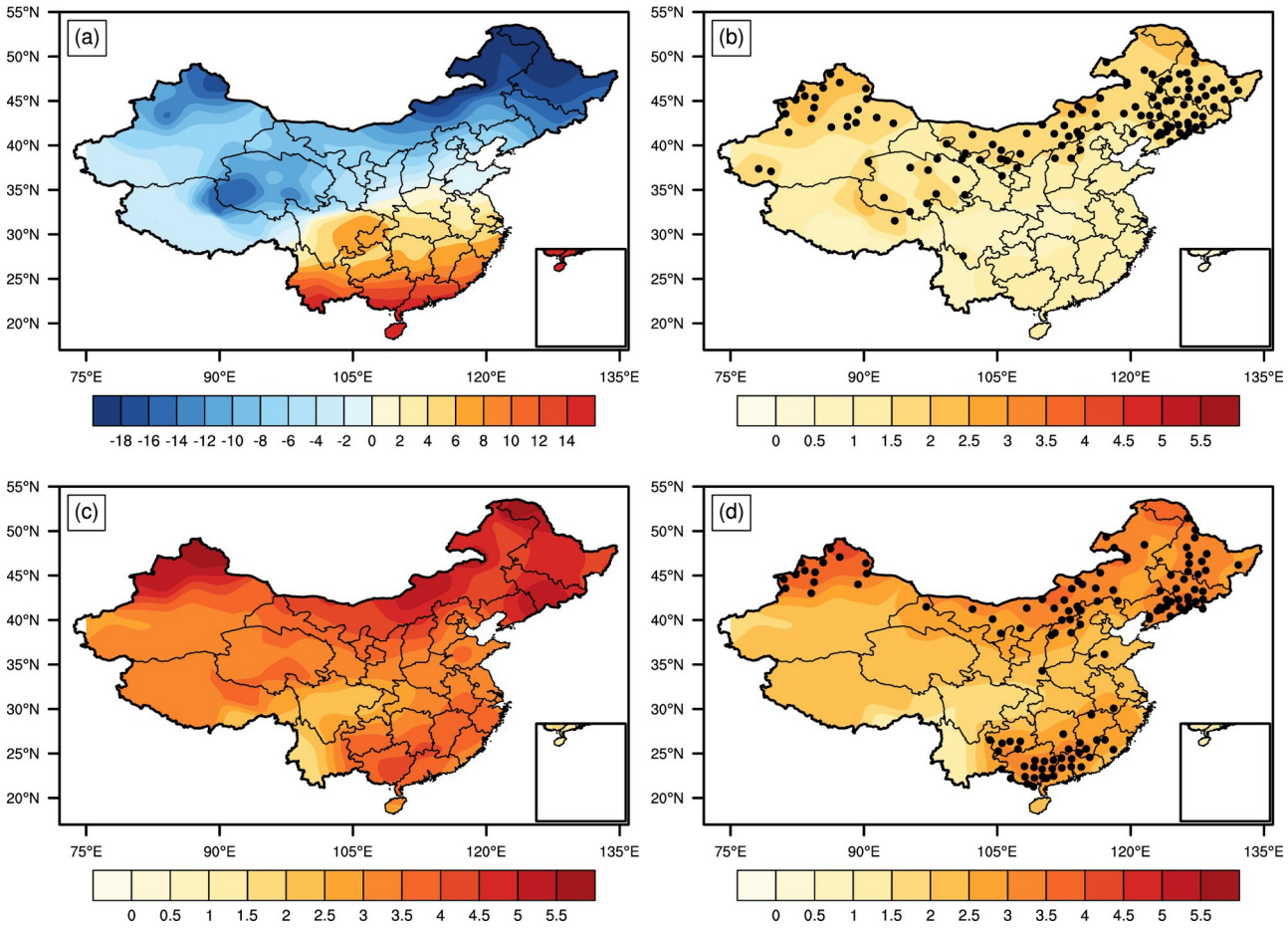

joc_7247_fig.1.eps

Author Manuscript

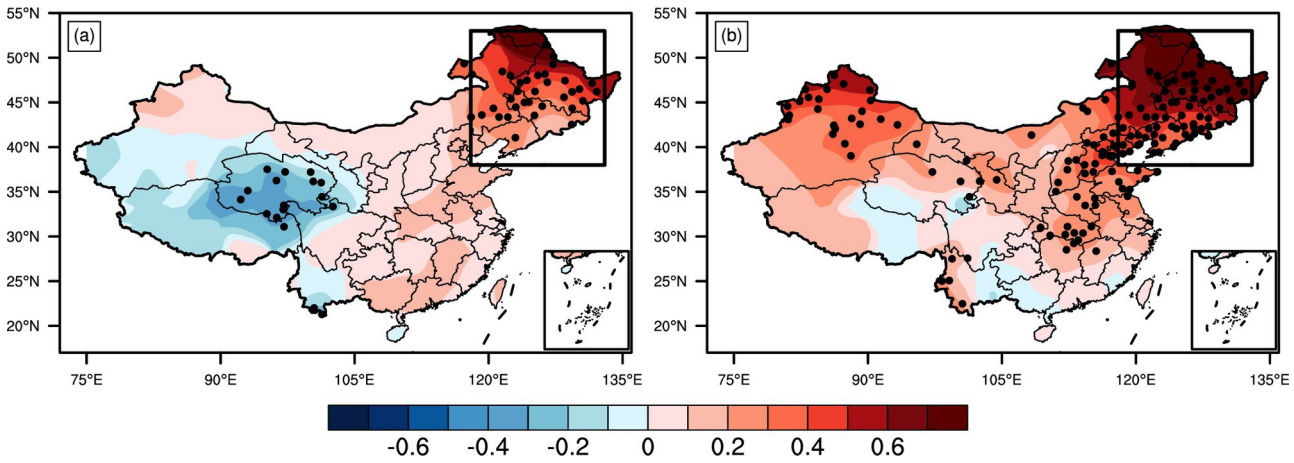

joc_7247_fig.2.eps

Author Manuscript

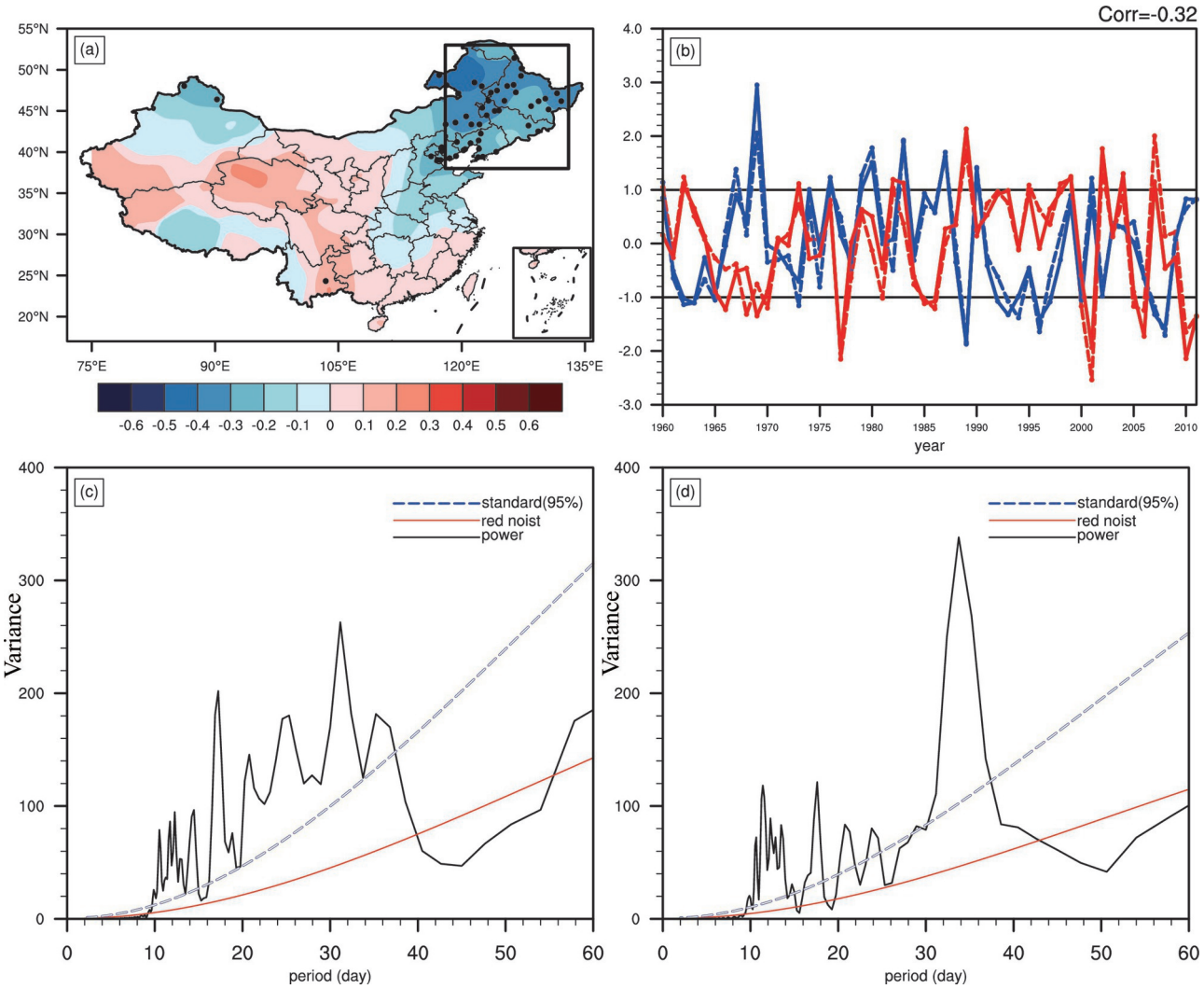

joc_7247_fig.3.eps

Author Manuscript

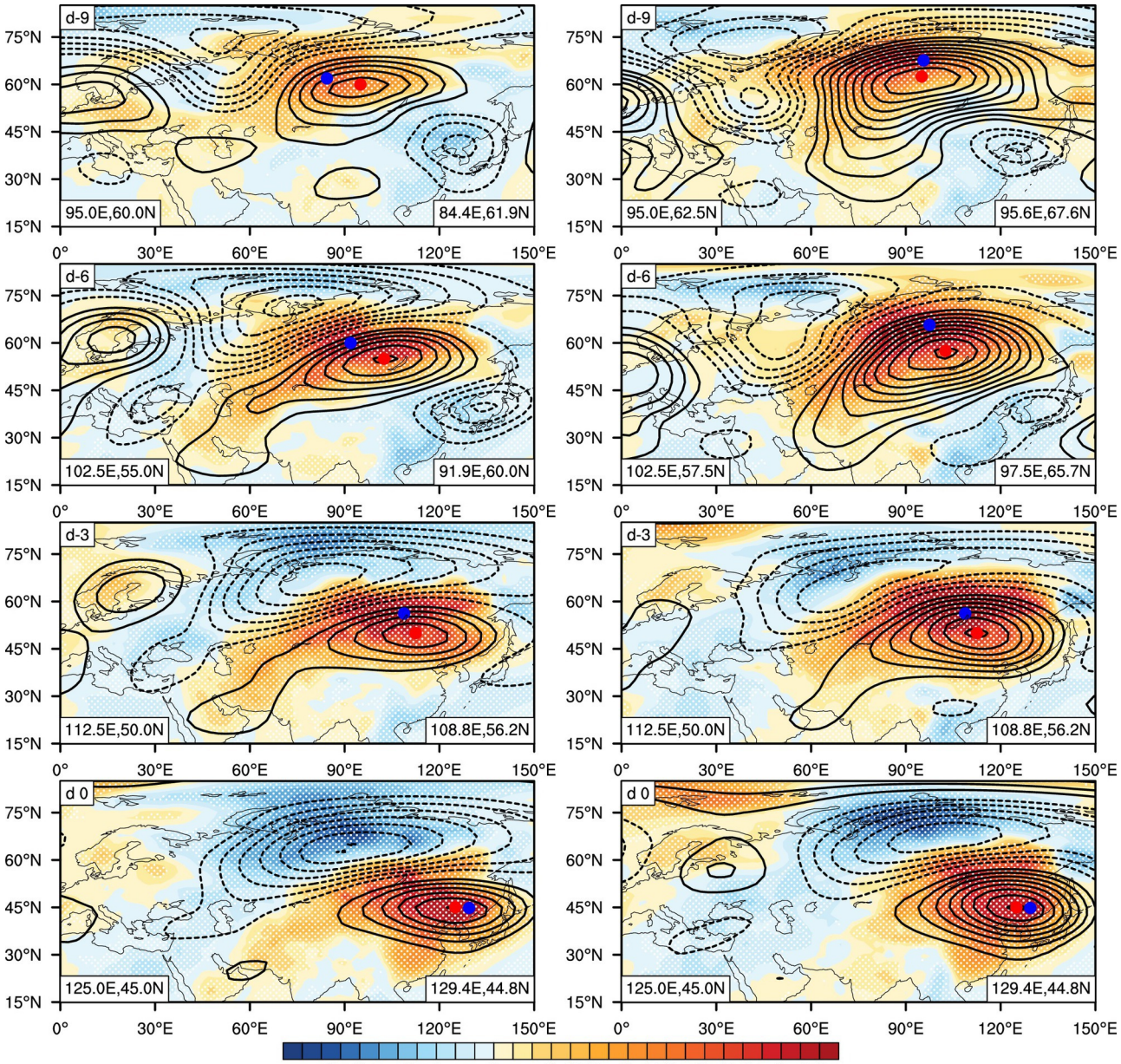

joc_7247_fig.4.eps

Author Manuscript

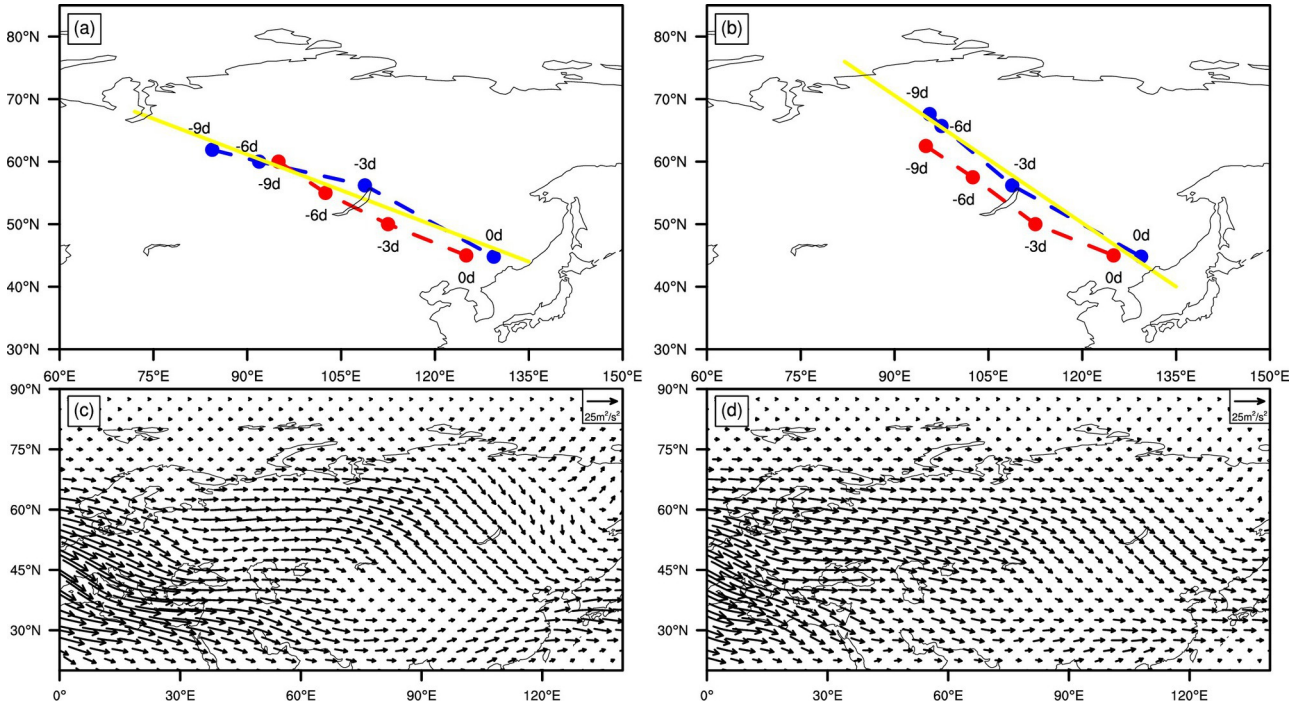

joc_7247_fig.5.eps

Author Manuscript

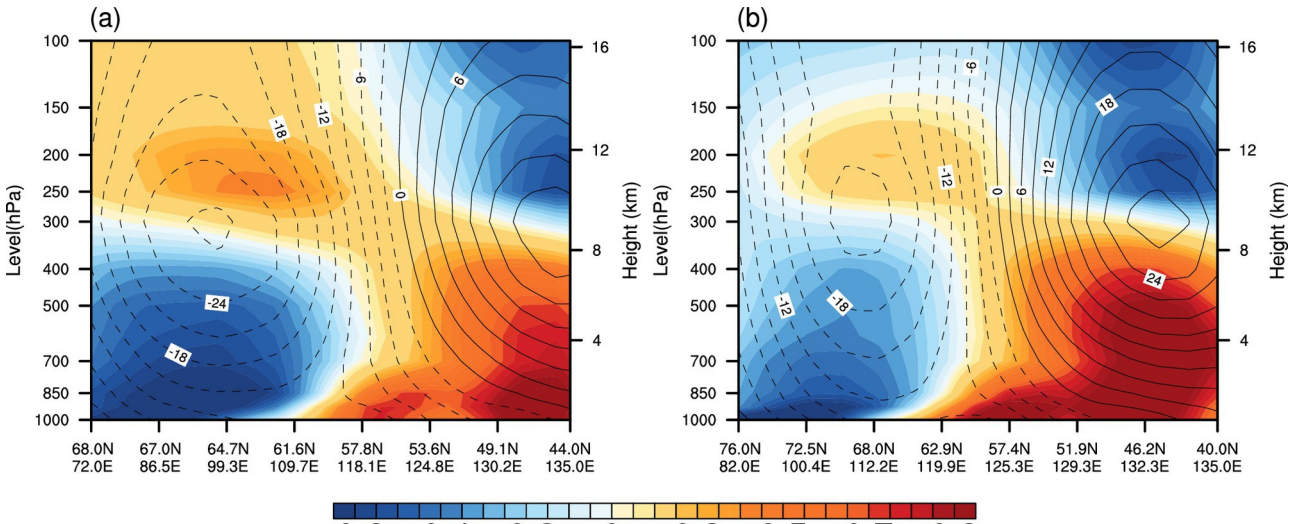

joc_7247_fig.6.eps

Author Manuscript

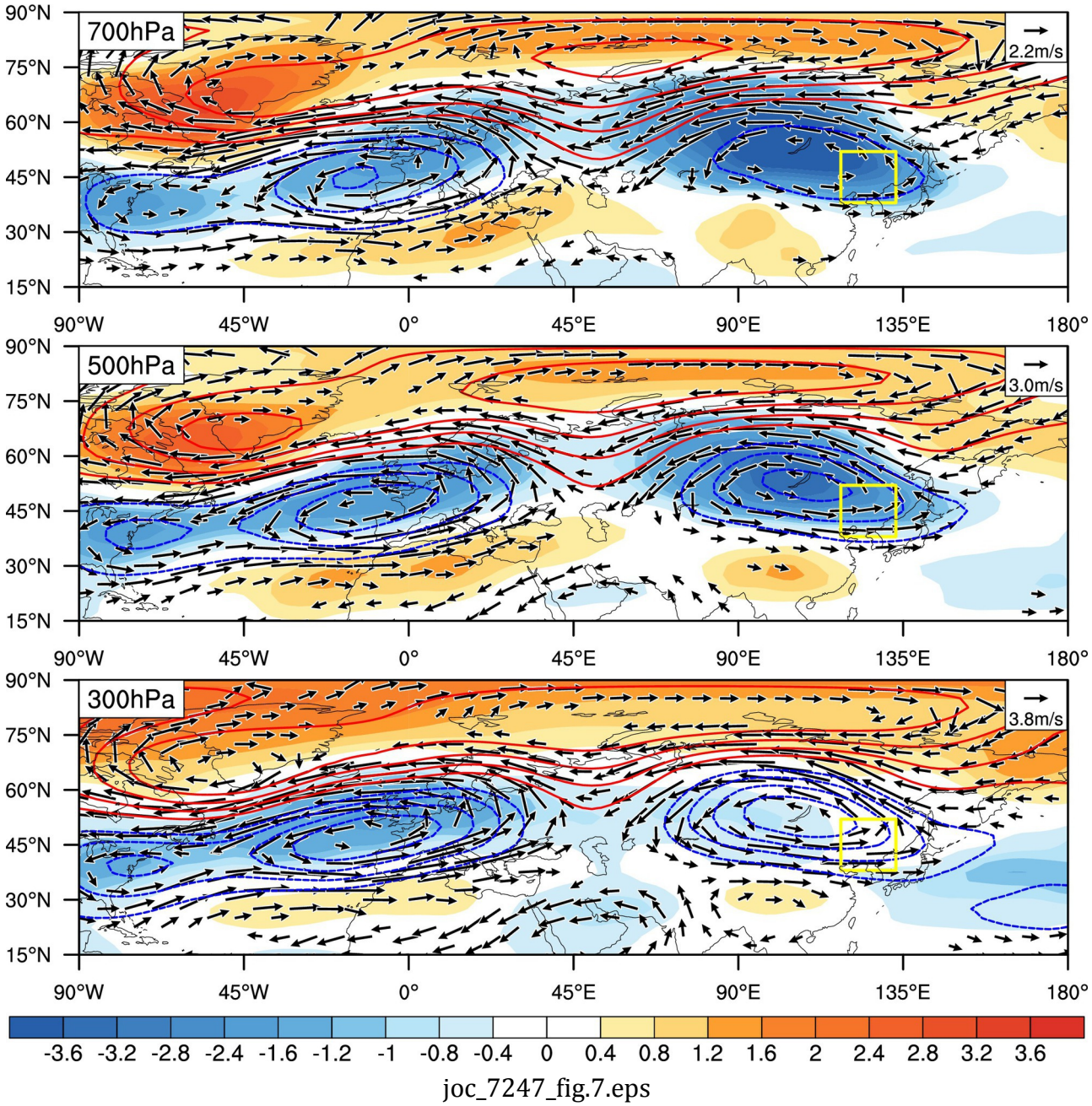

joc_7247_fig.7.eps

Author Manuscript

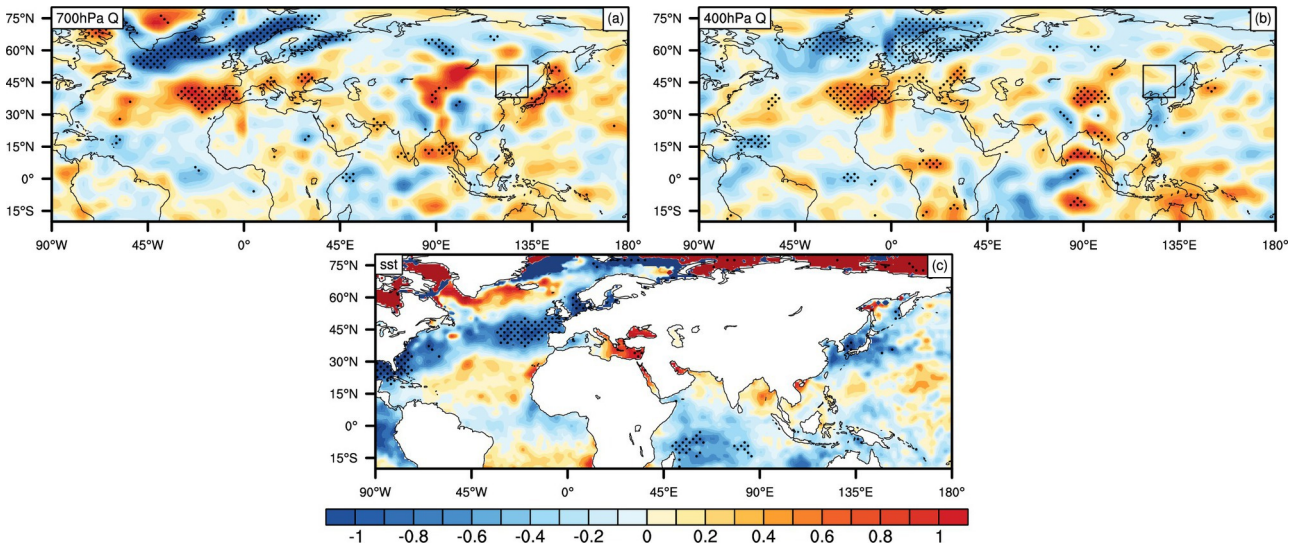

joc_7247_fig.8.eps

Author Manuscript

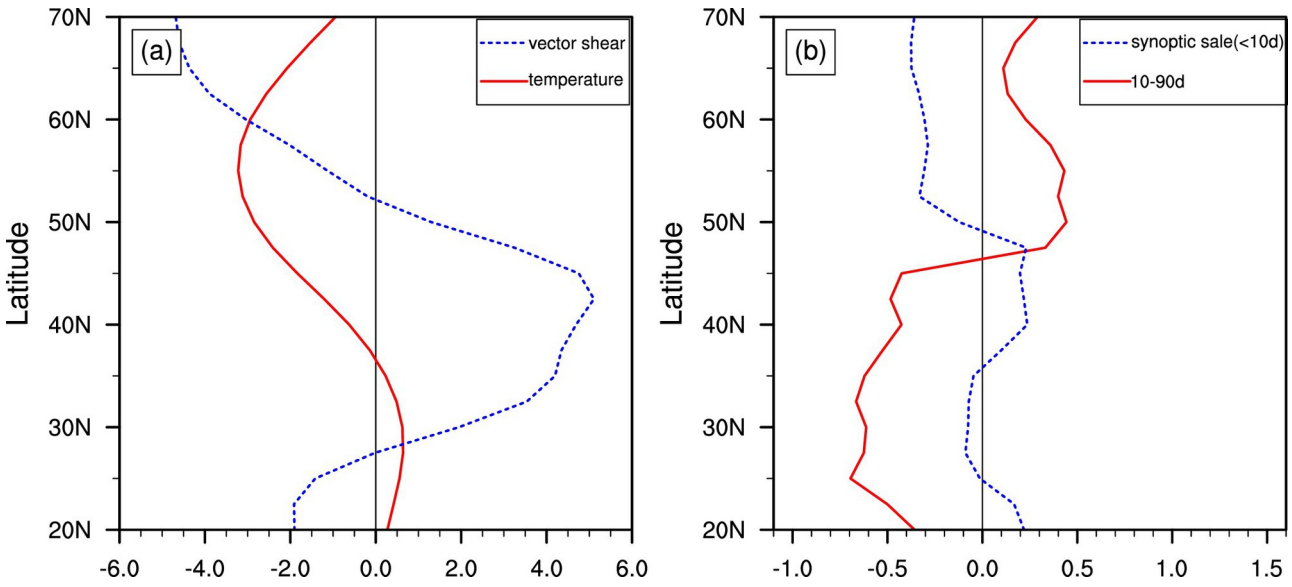

joc_7247_fig.9.eps

Author Manuscript

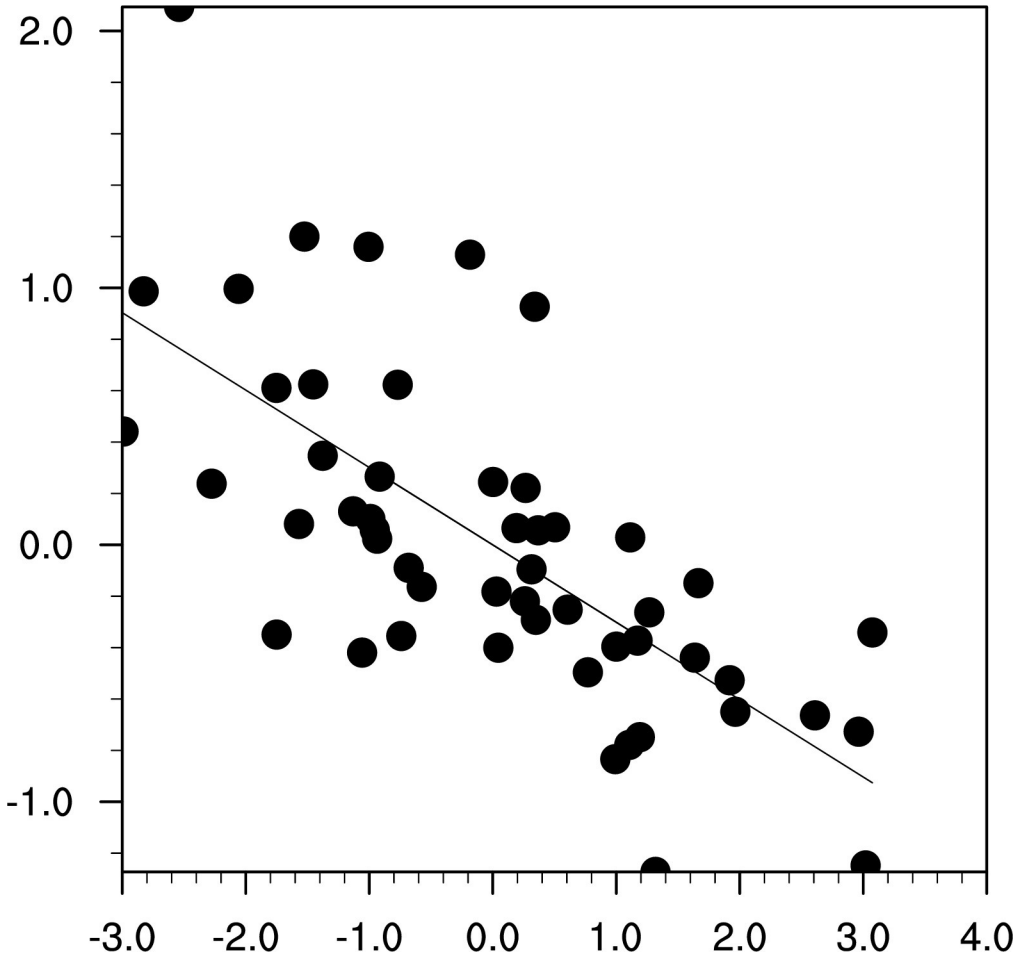

joc_7247_fig.10.eps

Author Manuscript

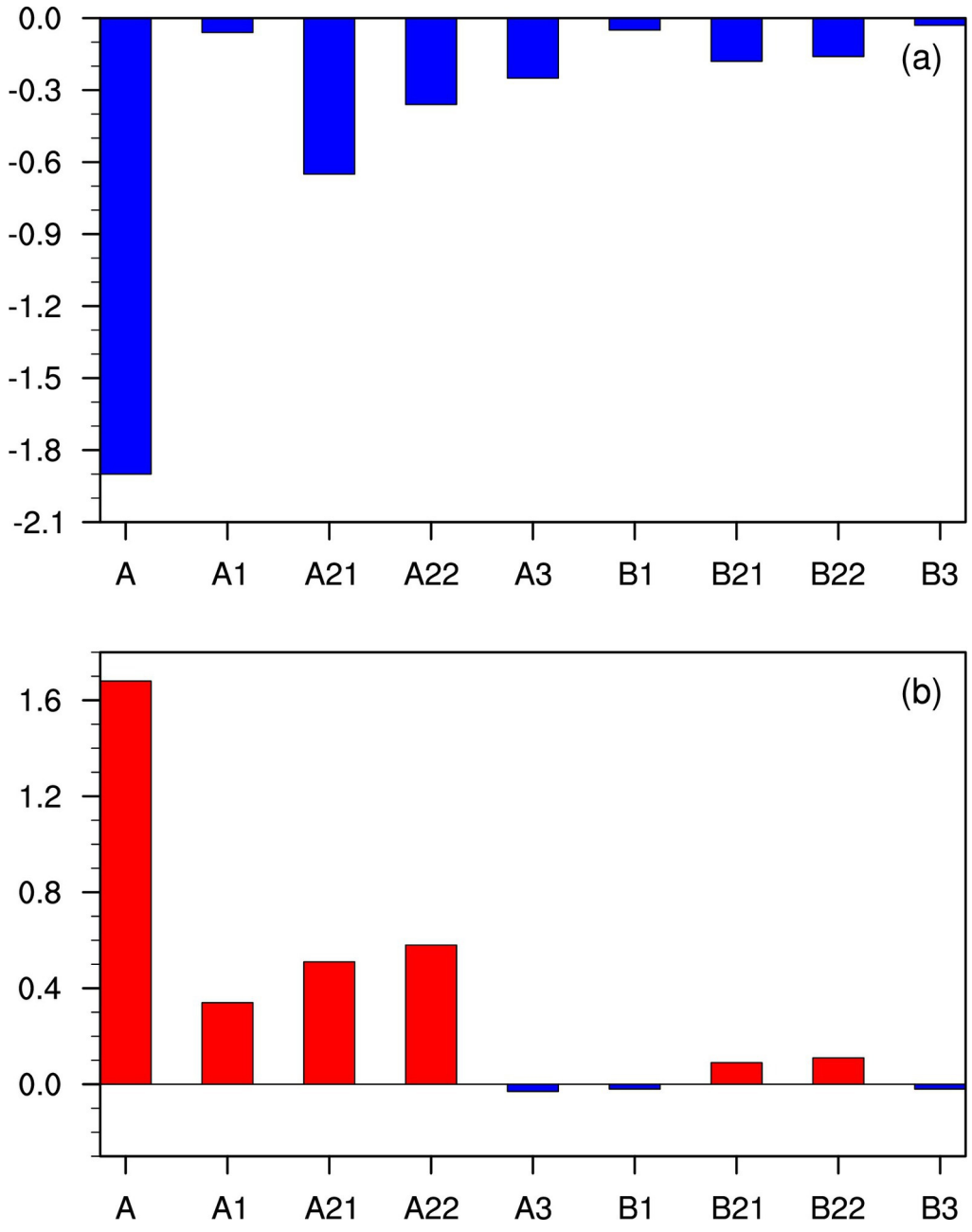

joc_7247_fig.11.eps

Author Manuscript

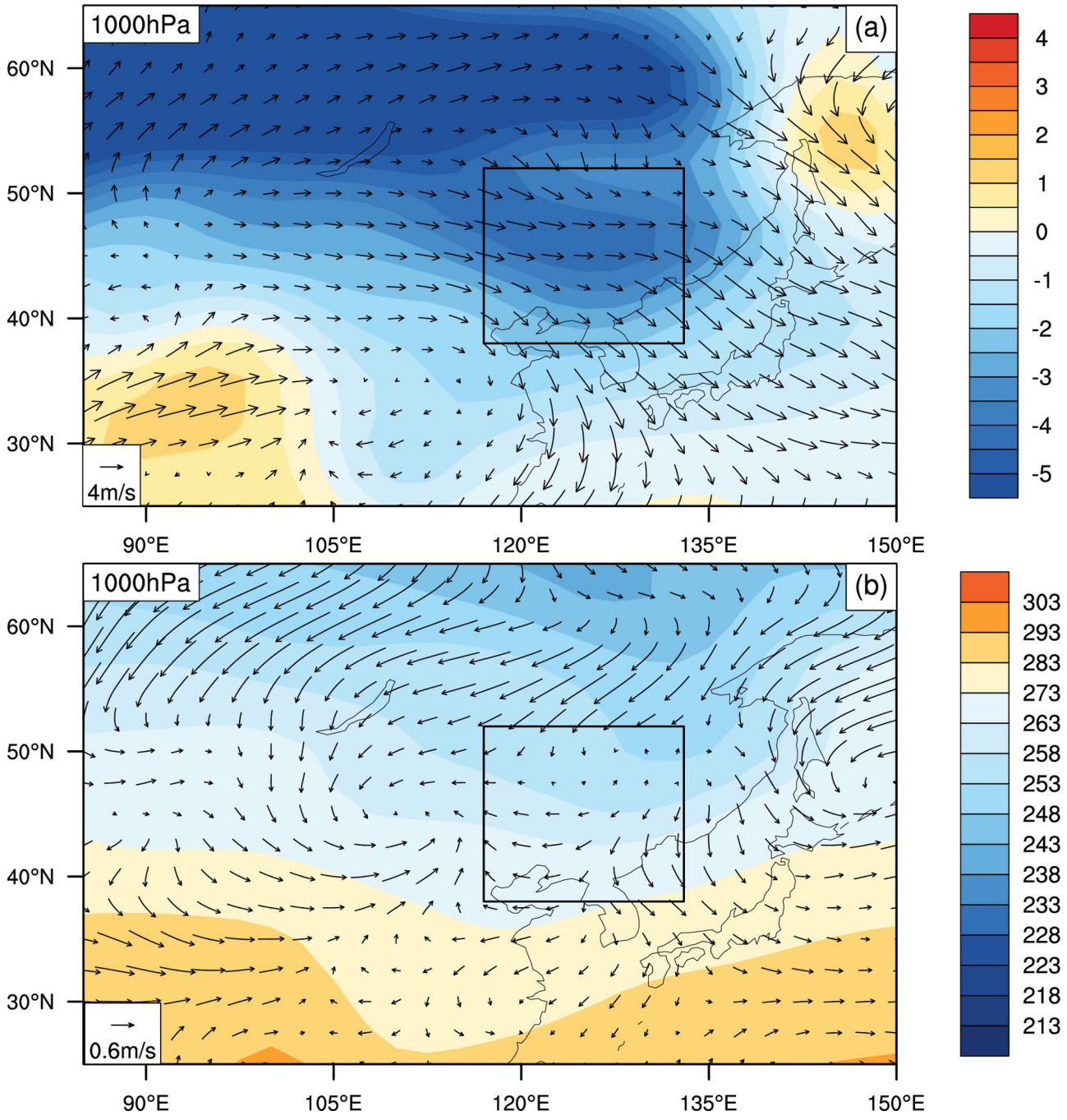

joc_7247_fig.12.eps

Author Manuscript

Relationship between the Interannual and Intraseasonal Temperature Variability in Northeast China

Wenhui Li[1,2], Guirong Tan[1], and Tim Li[3,1]

1. Key Laboratory of Meteorological Disaster, Ministry of Education (KLME) / Joint International Research Laboratory of Climate and Environmental Change (ILCEC) / Collaborative Innovation Center on Forecast and Evaluation of Meteorological Disasters (CIC-FEMD), Nanjing University of Information Science and Technology, Nanjing, 210044, China

2.Meteorological Public Service Center of Guangdong Province, Guangdong Province, Guangzhou, 510080, China

3.Department of Atmospheric Sciences, School of Ocean and Earth Science and Technology, University of Hawaii, Honolulu, Hawaii, HI96822, USA

Corresponding author: Tim Li, Department of Atmospheric Sciences, School of Ocean and Earth Science and Technology, University of Hawaii at Manoa, Honolulu, Hawaii 96822. Email: timli@hawaii.edu

Author Manuscript

Author Manuscript

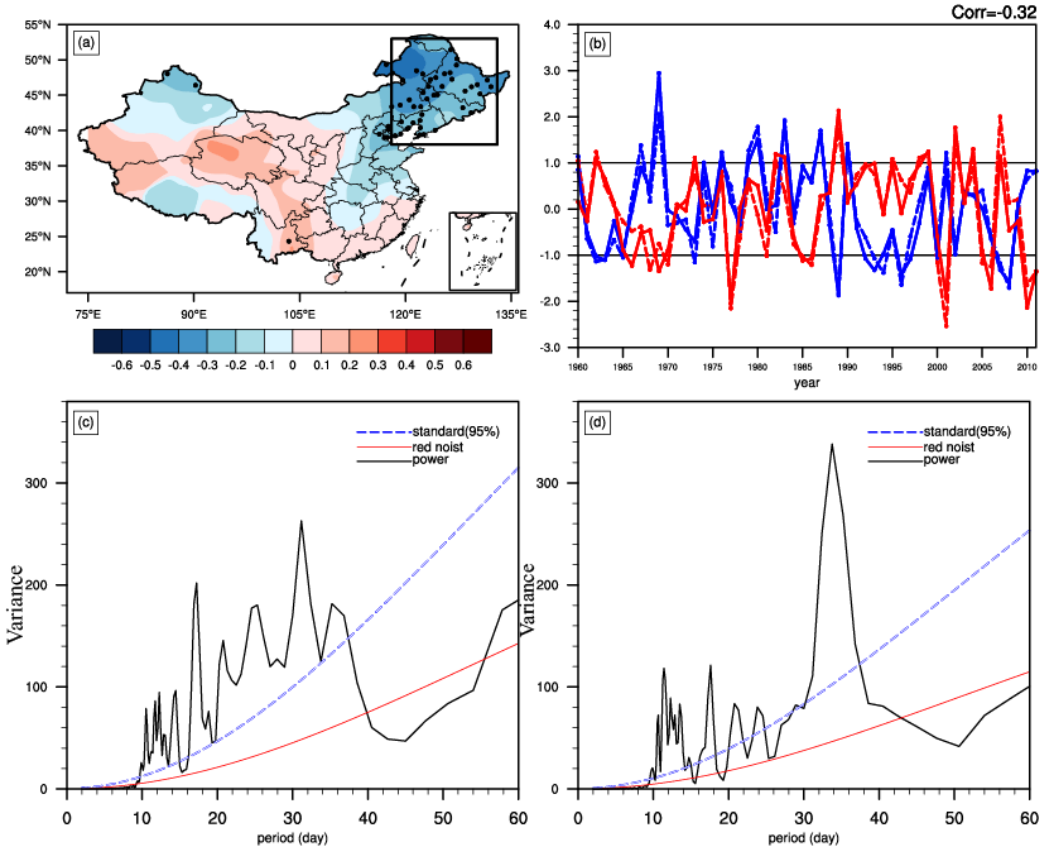

This work indicates that the correlation map between the time series of the ISO intensity averaged over 38-53°N, 118-133°E and the time series of the winter temperature anomaly at all stations. Significant negative correlations appear over Northeast China. The correlation coefficient between them is -0.32, exceeding the 95% confidence level. This indicates that a significant negative correlation occurs between the winter temperature anomaly and the ISO intensity in Northeast China. A stronger (weaker) ISO variability is accompanied with a cold (warm) winter over Northeast China.